Polish Society of Composite Materials
Polskie Towarzystwo Materiałów Kompozytowych

23: 3 (2023) 118-122

COMPOSITES THEORY AND PRACTICE
ISSN: 2084-6096
ISSN (online): 2299-128X

Abbasali Saboktakin*, Hossein Safaei

Izmir University of Economics, Department of Aerospace Engineering, İzmir, Turkey
**Corresponding author: E-mail: abbasali.saboktakin@ieu.edu.tr*

Received (Otrzymano) 10.12.2022

AEROSPACE 3D TEXTILE PREFORM ANALYSIS: EXPERIMENTAL AND MESOMODELING

For the purpose of predicting how textile preforms affect the quality of the composite material and its performance, the stitched textile preform must be characterized. Experimental compaction analysis and finite element analysis of textile preforms are the main subjects of this paper. The formability parameters of a preform can be changed by the stitching process, according to research on the mechanical properties of preforms conducted during compression testing. The load-deformation response, which is depicted in detail, had the greatest influence on preform deformation. Less fiber bundle undulation in the plane direction and more stitching thread undulation in the thickness direction were observed during compression of the stitched preform, whereas the stitching thread improved the resistance of the preform to compression loading.

Keywords: textile preforms, mesomodeling, aerospace, composite, characterization

INTRODUCTION

High-quality composite materials have been utilized in space applications for many years, and are primarily used in satellite structures, manned spacecraft, and space launch vehicles [1, 2]. They are employed in a wide range of applications in launch vehicles such as solid rocket engines in addition to fuel and gas pressure vessels. Many composite materials are used as a thermal protection system for vehicles to re-enter the atmosphere [3, 4]. The literature states that aerospace companies like NASA, Boeing, and Airbus are attempting to develop huge transport planes that are more effective and efficient to operate [5, 6]. With blended wing body (BWB) fixed-wing aircraft, which have no lines dividing the wings from the main body of the aircraft, the abovementioned companies are seeking to replace existing commercial aircraft designs with tubular fuselages and attached wings with more efficient ones. The usage of fasteners and rivets in aircraft is drastically reduced when the fuselage is completely integrated and blended with the aircraft wings according to research on the design, production, and testing of stitched composite constructions [7]. Three-dimensional (3D) textile composite structures for aerospace applications have been developed to solve the drawbacks of two-dimensional (2D) laminate composites [8]. The following characteristics of 3D textile composites made out of 3D textile preforms can be designed and manufactured, which exhibit increased strength and stiffness in the thickness direction [9].

The manufacturing of textile preforms and the evaluation of their performance for cutting-edge aerospace applications both rely heavily on the deformation modes that happen in 3D preforms. Equation (1) indicates the relation between applied pressure P and fabric volume V, where the constant is influenced by Young's modulus E, mass m, density δ, and variable K of the fiber [10, 11]. The crimp value and fiber orientation have an impact on the value of K, but fiber diameter d_f has no bearing. The relationship between fiber volume fraction V_f and applied compressive pressure P is expressed in Equation (2). The bending rigidity and fiber orientation both have an impact on the constant k. The order in which fabric layers are stacked, the orientation of the fibers, and the volume of the fibers all have a enormous impact on how compressible a textile is. When fabricating textile composites using mold pressure, it is crucial to establish the resin flow pattern

$$P = \frac{a}{V^3} \quad \text{where } a = KE\left(\frac{m}{\delta}\right)^3 \qquad (1)$$

$$P = k\,(Vf)^n \qquad (2)$$

The intricate 3D stitched fabric geometry and the spatially dissimilar yarn characteristics can be modeled using the 3D finite element method [12, 13]. The development of suitable material models and a geometry description can, however, be tremendous challenges and no published studies on this subject are currently available [14]. Numerous studies concern the examination of textile deformations, but no comprehensive general modeling study has been conducted on the compression of 3D stitched preforms [15].

In the current work, preform compaction mechanisms are covered, and how stitched and unstitched preforms respond to applied compression loads in terms of geometrical variables is explored. In order to forecast thickness as a function of compression pressure, a finite element model is utilized, along with an experimental test based on pressure displacement. The significance of the geometrical and mechanical parameters of stitched preforms impacting compression behavior is highlighted the most. The ability of this method is demonstrated by applying it to a 3D stitched preform, notably in terms of anticipating the evolution of the reconfiguration of the textile fabric structure.

EXPERIMENTAL MATERIAL AND EQUIPMENT

In this research study, the 11 layers of woven fabric that made up the textile preforms were arranged in a quasi-isotropic arrangement. The textile material weighs 305 g/m^2. Using a 6-axis KUKA robot with a commercial tufting head, these textiles were stitched with twisted 240 Tex polyester thread. Compression tests on the preform specimens were carried out using an MTS testing apparatus with a load cell capacity of 100 KN. A diagram of the compression test performed by an MTS machine is shown in Figure 1. The stitched preform was compressed by an upper circular punch that was moved downward during the compression test setup. The punch automatically reversed direction when the compressive force reached the specified limit. Throughout the test procedure, the force and displacement were recorded. The punch movement occurred at a rate of 1 mm per minute. The maximum load was limited to 20 KN. The final thickness was determined to be the thickness at which the compressive force reached 20 KN, and for analytical purposes, a representative load/deflection response curve for compression testing was recorded.

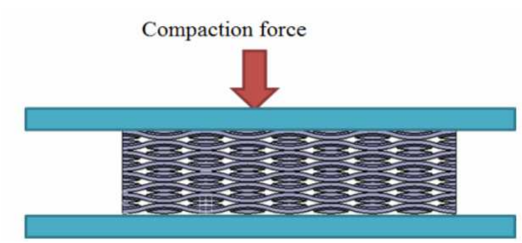

Fig. 1. Stitched preform compression test setup

Furthermore, the three-dimensional (3D) multiscale modeling approach allows more accurate modeling of the complex fabric geometry. In this procedure, the mechanical performance of the 3D textile composite is studied using the finite-element method to recognize the critical regions in which damage is probable to progress. Figure 2 presents the multiscale modelling of a stitched preform at the mesoscale. To explore the compacted textile geometry and assess its impacts on preform permeability and composite mechanical performance, a suitable unit cell simulation was run. The unit cells of the stitched and unstitched woven fabrics were discretized using appropriate elements, and rigid elements were employed for the compression platens.

The unit cell model was placed between the platens. The upper plate was crushed at a constant rate of displacement, while the lower plate was completely restrained. The surface-surface technique defined several interactions between the yarns and the unit cell surfaces with the plates. The geometry, material properties, mesh creation, and boundary conditions were all completed in order to carry out the simulation.

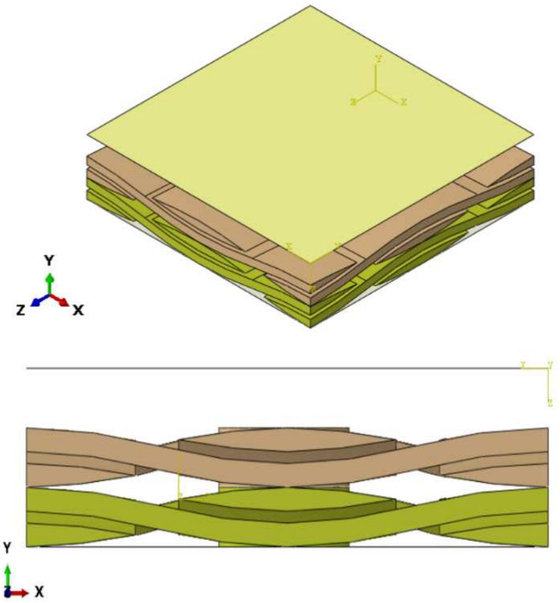

Fig. 2. Stitched preform unit-cell subjected to compression loading

The linear properties of a mesoscale elastic material were used to represent the textile preforms as a transversely isotropic component. The geometry of the fundamental weave structure was determined by measuring the actual sample, and Table 1 provides the characteristics of the woven textiles.

TABLE 1. **Material properties used in simulation [11]**

Textile fabric	G_{12} = 3.5 GPa E_{22} = 10.4 GPa X_T = 1140 MPa X_C = 620 MPa	G_{12} = 4.3 GPa ν_{12} = 0.28 Y_T = 39 MPa S_{12} = 89 MPa	E_{11} = 41 GPa ν_{23} = 0.5 Y_C = 128 MPa S_{23} = 89 MPa

Figure 3 displays the boundary conditions that were specified in the unit cell model. The unit cell was subjected to an applied pressure and slip boundary conditions were applied at the intersections of the fiber bundles. Periodic boundary conditions were employed in the X and Y directions, which are in-plane directions, while wall boundary conditions were applied along the Z direction, which is the through thickness direction.

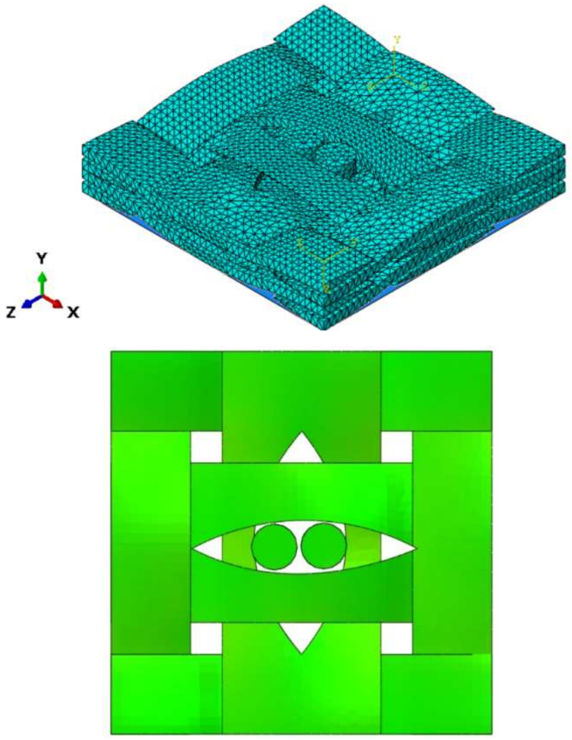

Fig. 3. Meshed model of stitched preform in mesoscale

RESULTS AND DISCUSSION

Figure 4a presents the pressure curves for stitched and unstitched preforms. The features of the stitched preforms were identical to those of the unstitched ones. Comparing the stitched preforms to the non-stitched preforms, the stitched preforms had the highest loading values at the same displacement.

Figure 4b shows the compression behavior force against the displacement curves for the stitched and unstitched preforms. Our results obviously demonstrate that the modelling approach is very suitable for anticipating any preform changes in the thickness direction as well as the mechanical response during compression. The stitched preform subjected to compressive pressure during modeling may have a slight variation, such as a sharp rise in force brought on by thread misalignment or bending across the thickness.

Figure 5 displays the simulated deformed unit cells for the unstitched and stitched preforms. The compression of an unstitched preform created stress in a small region that comes into contact with the upper platen. The two yarns of a cross-section of a yarn first formed a flat zone, which deformed the cross-section and compacted the yarns.

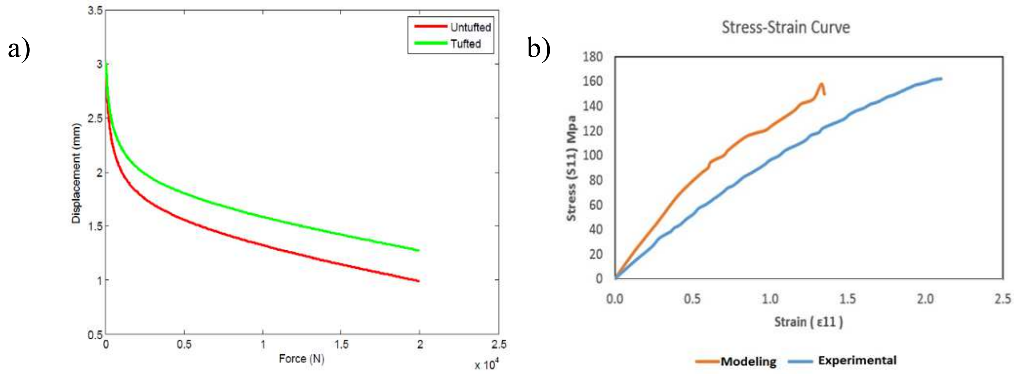

Fig. 4. Compression loading applied to preforms: a) load vs. displacement of stitched and unstitched performs, b) stress vs. strain plot of stitched preform

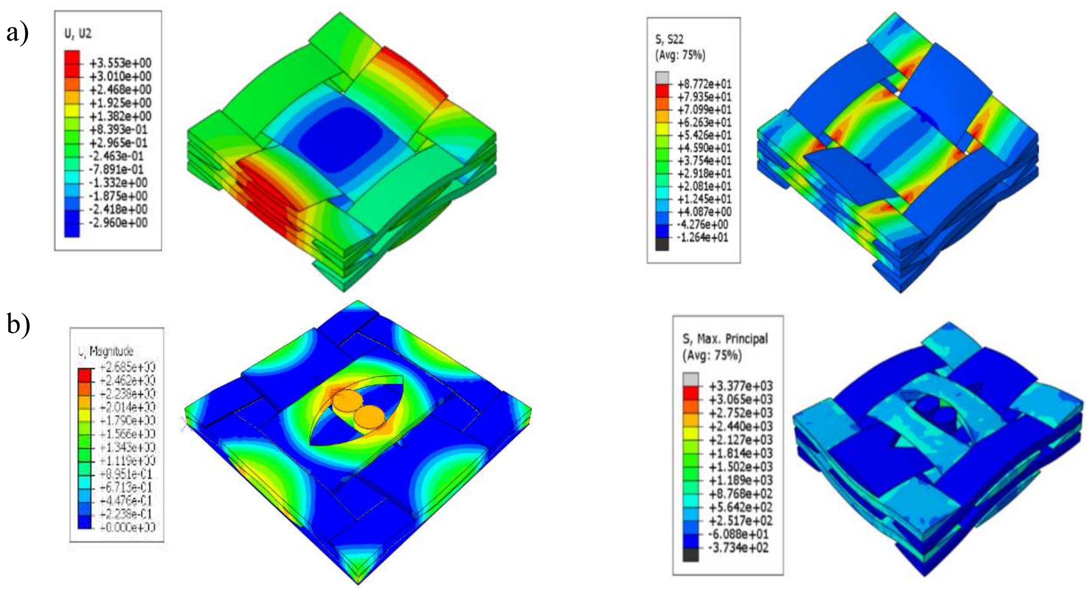

Fig. 5. Stress and displacement contours of: a) unstitched and b) stitched preform unit cells

The overall compressive load-bearing capacity of the preform is shown in Figure 6 by the application of localized compressive pressure to a small area of yarn crossovers in the stitching area. When compared to other parts of the fabric, the fiber volume fraction is the greatest and the cross-sectional area is the smallest at these points.

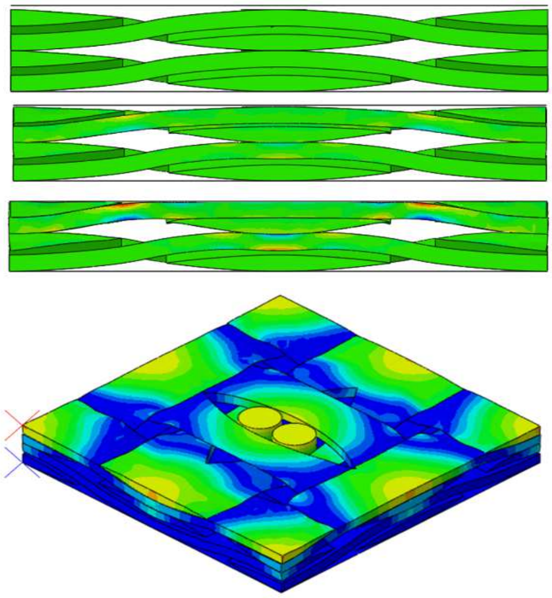

Fig. 6. Stitched preform deformation under compression loading: a) sequence of preform deformation, b) stress contour of stitched composite

In this study, it was found that a multiscale modeling technique can be used to precisely replicate the geometry and constitutive behavior of textile assemblies. Experimental testing was conducted to determine the accuracy of the simulation results for two-layer textiles. The domain size, fiber length, fiber quality, restrictions, and boundary conditions were among the factors that were investigated. The modeling enables a complete understanding of the behavior of the stitched textile preforms and the deformation they encounter under compression loading. The number of threads and fibers in actual preforms might reach hundreds. Nevertheless, only a few fibers were used to demonstrate the principle and potential of the approach. A large variety of different textile structures have been subjected to multiple, complex loading scenarios that can be simulated using the developed finite element modeling techniques. One of the key advantages of the finite element modelling of a unit cell compression model over other approaches is its capacity to record the most important preform properties when the preform is under compressive pressure. Nonlinear geometric and nonlinear preform characteristics should be modelled the most. Fiber bundle compaction and its bending deformations are the main variables influencing compaction behavior. These findings might have an impact on the development of analytical models, and ultimately, stitched textile preform design. Even though the model presented here is capable of capturing the most important responses of a unit cell to compressive pressure, the yarn was characterized as a continuum solid body, which is unable to effectively capture true yarn deformation mechanisms as a yarn is made up of many filaments. Meso-bending, shearing, and cross-section compaction all have a significant impact on how the yarn behaves. As a group, the authors are now doing research on the micro-modeling of stitched textile preforms.

CONCLUSION

Experimental analysis and a mesomodeling approach were used to characterize the compression test of stitched preforms. According to our findings, the fiber bundle underwent greater undulation in the thickness direction and less in the plane direction as a result of compression of the stitched preform, while the stimulation of the preform to start applying pressure was produced by the stitching thread. Because the fiber bundles flattened and the fiber crimp decreased when compression stress was applied to the preforms, the fiber volume fractions grew. During the compression test, the energy absorption in the stitched preform was found to be high.

REFERENCES

[1] Reinhart J., Overview of Composite Materials, [in:] Handbook of Composites, Springer, 1998.

[2] Ivanov D.S., Lomov S., Modelling the structure and behaviour of 2D and 3D woven composites used in aerospace applications, Polymer Composites in the Aerospace Industry, Woodhead Publishing, 2014.

[3] Deconinck P., Abdulhamid H., Héreil P., Experimental and numerical study of submillimeter-sized hypervelocity impacts on honeycomb sandwich structures, J. Procedia Engineering 2017, 204, 452-459.

[4] Riedel W., Nahme H., White D.M., Clegg R., Hypervelocity impact damage prediction in composites: Part II, experimental investigations and simulations, J. Impact Eng. 2006, 33(1-12), 670-680.

[5] NASA Contractor Report, Final Report for Contract NNL13AA11C, 218149, 2104.

[6] Tomich A., Clarke S., Integration of Complex Geometry, 3D Woven Preforms via Innovative Stitching Technique, Phase II, Space Technology Mission Directorate, NASA, 2019.

[7] Thrash P., Manufacturing of a Stitched Resin Infused Fuselage Test Article, CAMX SAMPE, 2014.

[8] Unal P.G., 3D Woven Fabrics, [in:] Woven Fabrics, IntechOpen 2012.

[9] Barile C., Casavola C., Pappalettere H., The influence of stitching and unconventional fibres orientation on the tensile properties of CFRP laminates, Compos. Part B Eng. 2017, 110, 248-254.

[10] Advani S.G., Murat S., Process Modeling in Composite Manufacturing, CRC Press, 2010.

[11] Simacek P., Advani S.G., Resin flow modeling in compliant porous media: An efficient approach for liquid composite molding, International Journal of Material Forming 2018, 11, 503-515.

[12] Pierreux G., Van-Hemelrijck D., Massart T., RVE computations for evaluation of microdamage initiation in structural stitched non-crimp fabric composites, Journal of Composite Materials 2020, 30, 4751-4771.

[13] Iwata A., Inoue T., Naouar N., Boisse P., Lomov V., Coupled meso-macro simulation of woven fabric local deformation during draping, Composites Part A: Applied Science and Manufacturing 2019, 118, 267-280.

[14] Huang J., Hamila N., Boisse P., Draping modelization of stitched composite reinforcements, ESAFORM, 26 August 2021.

[15] Shen H., Wang P., Legrand X., Liu L., Soulat D., Influence of the tufting pattern on the formability of tufted multi-layered preforms, Compos. Struct. 2019, 228, 111356.